Carbohydrate Polymers 79 (2010) 590–596

Contents lists available at ScienceDirect

Carbohydrate Polymers

journal homepage: www.elsevier.com/locate/carbpol

Chitosan–DNA–rectorite nanocomposites: Effect of chitosan chain length and glycosylation

Xiaoying Wang [a,b,1], Sabina P. Strand [b,*], Yumin Du [a], Kjell M. Vårum [b]

[a] Department of Environmental Science, College of Resource and Environmental Science, Wuhan University, Wuhan 430079, China
[b] Norwegian Biopolymer Laboratory (NOBIPOL), Department of Biotechnology, Norwegian University of Science and Technology (NTNU), Sem Saelands v. 6-8, N-7491 Trondheim, Norway

ARTICLE INFO

Article history:
Received 14 April 2009
Received in revised form 22 June 2009
Accepted 11 September 2009
Available online 18 September 2009

Keywords:
Chitosan
Rectorite
Nanocomposite
DNA
Gene transfection

ABSTRACT

Two fully deacetylated chitosans with low- and high molecular weight (LMW and HMW) and their glycosylated derivatives substituted with the trimer GlcNAc–GlcNAc–Mannose (AAM) were intercalated into rectorite to prepare polymer/clay nanocomposites. The interlayer distance of rectorite depended on the amount of chitosan and the structure of intercalated chitosan. The largest interlayer distance of 3.35 nm was obtained when the mass ratio of LMW non-substituted chitosan to rectorite was 2:1. The four chitosan–rectorite nanocomposites were loaded with DNA and their dispersion stability and DNA retention capability were evaluated. Similarly as for DNA–chitosan polyplexes, the colloidal stability of the chitosan–DNA–rectorite nanocomposites increased with the increasing molecular weight of the intercalated chitosan and was improved by glycosylation. The nanocomposite of HMW and glycosylated chitosan did not aggregate in phosphate buffered saline (PBS) at pH 7.4 and retained a size of approximately 200 nm diameter. The DNA retention capability of the nanocomposites was also dependent on the structure of the intercalated chitosan. Nanocomposites based on the LMW and glycosylated chitosan required high amount of the polymer (corresponding to amino: phosphate ratio of 60) to retain the loaded DNA. The in vitro transfection study revealed that the chitosan/rectorite composites were able to deliver DNA to human cells, albeit with reduced efficacy compared to chitosan/DNA nanoparticles.

1. Introduction

Biopolymer–clay nanocomposites have recently attracted much attention, exhibiting remarkable improvements of material properties when compared to clay or polymers alone (Viseras et al., 2008; Zeng & Yu, 2008). Clay materials have been extensively applied for drug delivery due to the good intercalation capacity of the clay particles (Aguzzi, Cerezo, Viseras, & Caramella, 2007). Clay minerals such as montmorillonite, illite, and kaolinite are well known to protect DNA from nucleases during natural bacterial genetic transformation (Demaneche, Jocteur-Monrozier, Quiquampoix, & Simonet, 2001; Lin, Chen, Cheng, & Kuo, 2006). The transformational ability of clay is believed to play a role in evolution and genetic exchange among unrelated organisms (Kawase et al., 2004). Clay minerals have already been used safely in human applications, such as anti-diarrheal medicine, antacids, and cosmetics (Aguzzi et al., 2007). Rectorite (REC) is a regularly interstratified clay mineral with alternate pairs of dioctahedral mica-like layer (nonexpansible) and dioctahedral montmorillonite-like layer (expansible) in a 1:1 ratio.

To modify or improve the affinity of the natural clays for the bioactive molecules, such as DNA, polymers may be added. Although various polymers have been used in polymer–clay composites, biopolymers are particularly interesting for drug and gene delivery applications.

Cationic polymers which condense plasmid DNA (pDNA) through electrostatic interactions to form polyplexes have emerged as safer, though less efficient, options for gene transfer (Montier, Benvegnu, Jaffres, Yaouanc, & Lehn, 2008). Chitosans, a family of cationic and linear polysaccharides derived from chitin, have been employed as polycationic carriers for pDNA in gene delivery systems with promising results (Kim et al., 2007). As generic chitosans are only soluble at pH-values below 6 and will precipitate upon increase of pH to neutral values (Varum, Anthonsen, Grasdalen, & Smidsrod, 1991), their application in biological systems at physiological pH is challenging. To overcome this obstacle, different derivatives of chitosan have been prepared. Glycosylation of chitosan was shown to improve the colloidal stability of the formulation as well as gene delivery efficacy (Hashimoto, Morimoto, & Saimoto, 2006; Issa et al., 2006; Strand, Issa, Christensen, Varum, & Artursson, 2008).

* Corresponding author. Tel.: +47 7359 4069; fax: +47 7359 1283.
E-mail address: sabina.strand@biotech.ntnu.no (S.P. Strand).
[1] Present address: State Key Laboratory of Pulp and Paper Engineering, School of Light Industry and Food, South China University of Technology, Guangzhou 510640, China.

0144-8617/$ - see front matter © 2009 Elsevier Ltd. All rights reserved.
doi:10.1016/j.carbpol.2009.09.012

It has been suggested that a key to successful transfection with chitosan is to achieve a subtle balance between DNA protection and intracellular DNA release (Koping-Hoggard et al., 2004; Strand, Danielsen, Christensen, & Varum, 2005). Consequently, all variables that affect the stability of polyplexes such as chain length, the fraction of acetylated units (F_A), glycosylation and so on were found to influence gene transfer efficacy (Issa et al., 2006; Koping-Hoggard et al., 2004; Romoren, Pedersen, Smistad, Evensen, & Thu, 2003; Strand et al., 2008).

Chitosan has also been extensively used in combination with inorganic materials such as gold (Liu, Chen, & Liu, 2008; Liu, Peng, Yang, Wu, & He, 2008), TiO_2 (Yuan, Venkatasubramanian, Hein, & Misra, 2008), Fe_3O_4 (Yuan, Ji, Fu, & Shen, 2008; Yuan, Venkatasubramanian, et al., 2008) and clay (Liu, Chen, et al., 2008; Liu, Peng, et al., 2008; Wang, Du, & Luo, 2008; Wang, Pei, Du, & Li, 2008). Liu (Liu, Chen et al., 2008) reported drug release behavior of chitosan–montmorillonite nanocomposite hydrogels following electrostimulation. In our previous study (Wang, Du, et al., 2008; Wang, Pei, et al., 2008), quaternized chitosan/montmorillonite nanocomposite nanoparticles were prepared, and it was found that certain montmorillonite loadings on quaternized chitosan can enhance the drug encapsulation efficiency and decrease the drug release rate. Also, our previous study revealed that REC is nontoxic to cells and can be used as a non-viral gene delivery system after the combination with quaternized chitosan (Wang, Du, et al., 2008; Wang, Pei, et al., 2008). As the nanocomposites are known to combine the physical and chemical properties of both inorganic and organic material, we sought to combine the advantages of the trisaccharide-substituted chitosan with rectorite.

In this study, we have prepared and characterized four different chitosan–rectorite nanocomposites, where both the structure and amount of intercalated chitosans were varied. Specifically, we have compared nanocomposites based on two fully deacetylated chitosan (low/high molecular weight) and their 2-acetamido-2-deoxy-β-D-glucopyranosyl-(1 → 4)-2-acetamido-2-deoxy-β-D-glucopyranosyl-(1 → 4)-2,5-anhydro-D-mannofuranose(A-A-M) substituted analogues. After characterization, we loaded the nanocomposites with DNA and compared their dispersion stability and DNA retention ability. Finally we have investigated the transfection efficacy of chitosan–DNA–rectorite nanocomposites and compared them with DNA–chitosan polyplexes.

2. Experimental

2.1. Materials

Three fully deacetylated chitosans ($F_A < 0.001$ as determined from their proton NMR-spectra (Varum et al., 1991) were prepared by heterogeneous de-N-acetylation of shrimp chitin as previously described (Ottøy, Vårum, & Smidsrød, 1996), converted to HCl salts, and lyophilized. The measured intrinsic viscosity (η)-values of the chitosans at pH 4.5 and ionic strength 0.1 M were: 49, 220 and 440 ml/g. The molecular weights (M_w) and molecular weight distributions were analyzed by size-exclusion chromatography with refractive index (RI) and a multiangle laser light scattering detector (SEC–MALLS). All samples were dissolved in MQ water (5–7 mg/ml) and filtered through 0.22 μm syringe filter (Millipore). The column used was TSK 3000, and sample was eluted with 0.2 M ammonium acetate (pH 4.5) at a flow rate of 0.5 mL/min. For simplicity, the three chitosans are denoted as ChLo (M_w 20 kDa), ChMe (M_w 67 kDa) and ChHi (M_w 146 kDa). The characteristics of the chitosans used in the study are given in Table 1. Calcium rectorite (Ca^{2+}-REC) refined from the clay minerals was provided by Hubei Mingliu Inc. Co. (Wuhan, China). Sodium nitrite, ammonium acetate and sodium cyanoborohydride were obtained from Merck.

Table 1
Characterization of chitosans used in this study. Intrinsic viscosity [η], molecular weight (M_w), polydispersity index (PDI) and degree of substitution (d.s.).

Sample	d.s. (%)	[η] ml/g	M_w (g/mol)	PDI (M_w/M_n)
ChLo		49	20,000	1.7
ChMe		220	67,000	1.5
ChHi		440	146,000	1.7
TriChLo	9.3			
TriChHi	8.6			

D_2O (99.96% D atom) was purchased from Isotech Inc. Agarose (A 9539) and ethidium bromide (EtBr, E 1510) were purchased from Sigma–Aldrich DNA. The plasmid pBR322 (~4.4 kbp, Promega) was used in this study.

2.2. Preparation of fully N-acetylated trimers

The trimer 2-acetamido-2-deoxy-β-D-glucopyranosyl-(1 → 4)-2-acetamido-2-deoxy-β-D-glucopyranosyl-(1 → 4)-2,5-anhydro-D-mannofuranose (A-A-M) was prepared as earlier described (Tommeraas, Varum, Christensen, & Smidsrod, 2001). The oligomers were separated by size-exclusion chromatography (SEC).

2.3. Preparation of trimer-substituted chitosan

Two of the chitosans (ChLo and ChHi) were substituted by reductive N-alkylation with the trimer A-A-M as previously described (Tommeraas et al., 2002). The characterization of the trimer-substituted chitosans using ^1H NMR spectroscopy revealed a degree of substitution (DS) of 9.3% and 8.6%. These chitosans are referred to as TriChLo (M_w 20 kDa) and TriChHi (M_w 146 kDa).

2.4. Quantification of chitosan adsorbed to rectorite

The REC sample was dispersed in distilled water and the clay suspension was left for 24 h after vigorous stirring for 30 min. Three chitosans were dissolved in water to obtain a 0.5% (w/v) solution, and were then added slowly into the REC suspension at the mass ratios of chitosan to rectorite of 0.1:1, 0.3:1, 0.5:1, 2:1 and 4:1. The adsorption proceeded at 60 °C for 2 days. The resulting solutions were centrifuged at 14,000 rpm for several times until no free chitosan in the supernatant was detected, and the sediments were collected and freeze-dried at −60 °C. Finally, the samples were applied to elemental analysis (C, N, H) on a Flash Elemental Analyzer 1112 (ThermoQuest, Milan, Italy) to determine the chitosan amount adsorbed on rectorite.

2.5. Preparation of chitosan/rectorite nanocomposites

The chitosan–rectorite nanocomposites were prepared as described above at the mass ratios of chitosan to rectorite of 1:1 and 2:1. The nanocomposites were freeze-dried at −60 °C and ground to powder. The overview of prepared nanocomposites and their designation is given in Table 2.

2.6. Characterization of chitosan/rectorite nanocomposites

The X-ray diffraction (XRD) experiment was performed using a D8 Advance diffractometer (Bruker, USA) with Cu target and Kα radiation ($\lambda = 0.154$ nm) at 40 kV and 50 mA. The scanning rate was 0.05°/min and the scanning scope of 2θ was 1–10° at room temperature.

Ultrathin films (50 nm) for transmission electron microscopy (TEM) analysis were prepared by cutting from the epoxy block with the embedded nanocomposites sheet at room temperature

Table 2
Chitosan–rectorite nanocomposites used in the study.

Nanocomposite designation	Intercalated chitosan	Chitosan:REC mass ratio
ChLo1REC	20 kDa	1:1
ChLo2REC	20 kDa	2:1
ChHi1REC	146 kDa	1:1
ChHi2REC	146 kDa	2:1
TriChLo1REC	20 kDa, AAM	1:1
TriChLo2REC	20 kDa, AAM	2:1
TriChHi1REC	146 kDa, AAM	1:1
TriChHi2REC	146 kDa, AAM	2:1

using an LKB-8800 ultratome. The TEM micrographs were taken using a transmittance electron microscope (JEM-2010 FEF (UHR), Japan) at an accelerating voltage of 200 kV.

2.7. Formulation of polyplexes and DNA loaded chitosan/rectorite nanocomposites

Stock suspensions (0.5 mg/ml) of chitosans and chitosan/rectorite nanocomposites were prepared in sterile MilliQ water. Chitosan polyplexes and chitosan–DNA–rectorite nanocomposites were formulated by adding pDNA stock solutions, and then chitosan or chitosan/REC to sterile MilliQ water during intense stirring on a vortex mixer (Heidolph REAX 2000, level 4, Kebo Lab, Sweden). The mixing ratio between chitosan or nanocomposites and DNA is expressed as the molar ratio between all protonable amino groups of chitosan and the phosphate groups of DNA and is referred to as the A/P ratio.

2.8. Size measurements

The mean hydrodynamic diameters (*z*-average) of polyplexes and chitosan–DNA–rectorite nanocomposites were determined by photon correlation spectroscopy on a Zetasizer Nano ZS (Malvern Instruments, Malvern, U.K.). The polyplexes and DNA-loaded nanocomposites were prepared at an A/P of 3 in water for size distribution. All measurements were carried out in triplicate at 25 °C and mean values were reported.

The time-dependent aggregation of the polyplexes and chitosan–DNA–rectorite nanocomposites was also studied in PBS of pH 7.4. The relative change in hydrodynamic diameter of the polyplexes and chitosan–DNA–rectorite nanocomposites (i.e. rate of aggregation) at the given time was estimated from the following equation: $(S_t - S_0)/S_0$, where S_0 and S_t represent the average diameter of the polyplexes and chitosan–DNA–rectorite nanocomposites measured immediately after formulation and at the given time (t), respectively.

2.9. Gel retardation assay

The DNA retention capacity of the nanocomposites was studied using the agarose gel electrophoresis, which was performed in 0.8% agarose gel in 40 mM Tris–acetate–EDTA (TAE) buffer at pH 8. The polyplexes and chitosan–DNA–rectorite nanocomposites at A/P ratios of 0.2–60 were prepared as described above at a constant DNA concentration of 13 μg/ml and incubated for 30 min. Next, 10 μl of the complex solution was mixed with 5 μl of loading buffer and loaded into the agarose gel wells. After electrophoresis (80 V, 45 min), the DNA was stained by incubating the gels in TAE buffer of pH 8 containing EtBr (0.5 μg/ml) for 15 min.

2.10. In vitro transfection

Human embryonic kidney cell line HEK293 was obtained from ATCC (Rockville, MD, USA). The HEK293 were grown in MEM (Gibco Invitrogen, cat. Nr. 31095) supplemented with 1 mM of non-essential amino acids and 10% fetal bovine serum (FBS, Gibco Invitrogen) at 37 °C and 5% CO_2. The cells were seeded in 96-well tissue culture plates (Corning Cell-bind #3300) 24 h prior to the transfection experiments to obtain cell confluency of 80–90% on the day of transfection. The polyplexes or DNA-loaded nanocomposites formulated in MQ water were diluted 1:2 by OptiMEM (OptiMEM I, Gibco Invitrogen) supplemented by 270 mM mannitol and 20 mM HEPES to adjust osmomolality and pH. Cells were washed with pre-heated OptiMEM and 50 μl of isotonic formulation containing 0.33 μg pDNA (pWizLuc, Aldevron) was added to each well. After 5 h of incubation, the formulations were replaced by 0.2 mL of fresh culture medium (MEM, 10% FBS). To determine luciferase expression, cells were washed twice with pre-heated PBS, lysed with luciferase lysis buffer (Promega) and the luciferase activity (RLU) was measured on a luminometer (Molecular Devices). The total cell protein was determined by bichinchoninic acid assay (Pierce).

3. Results and discussion

3.1. Adsorption of chitosan on rectorite

In this study, fully deacetylated chitosan (HCl salts) were used, and the adsorption of chitosan to rectorite was carried out in MQ water at low pH, when most of the amine groups were protonated. In such case, the adsorption process is controlled by the electrostatic interaction between the positive amino groups of chitosan and the negative sites in the rectorite structure as well as the cationic exchange between the amino groups of chitosan and the Ca^{2+}ions of rectorite interlayer (Usuk et al.,1993). In order to determine the amount of chitosan adsorbed on rectorite, the free unbound chitosan was removed by centrifugation and the content of nitrogen was determined by elemental analysis. As shown in Fig. 1, the amount of bound chitosan increased with increasing mass ratio of chitosan to rectorite up to the ratio of 2:1. Therefore, the nanocomposites with mass ratios of chitosan to rectorite of 1:1 and 2:1 were prepared and used in this study.

The effect of molecular weight of chitosan on the adsorbed amount of chitosan is shown in Fig. 2. The amount of chitosan bound to rectorite is relatively constant, with only slightly more chitosan with the highest and lowest molecular weight bound to rectorite as compared to the intermediate. Therefore, the chitosans

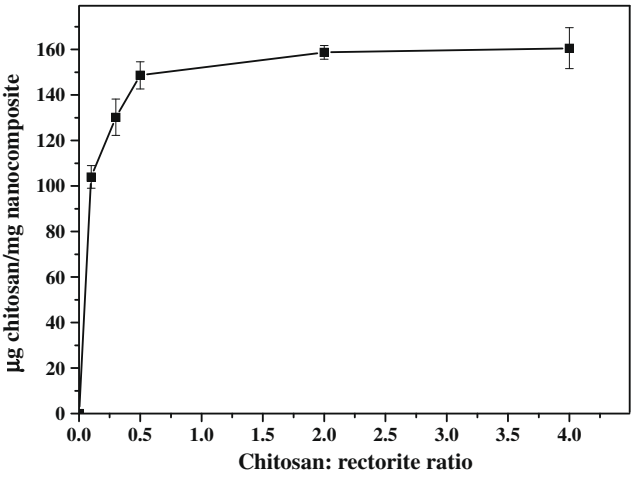

Fig. 1. Influence of the mass ratios of chitosan (M_w 67 kDa) to rectorite on the amount of bound chitosan.

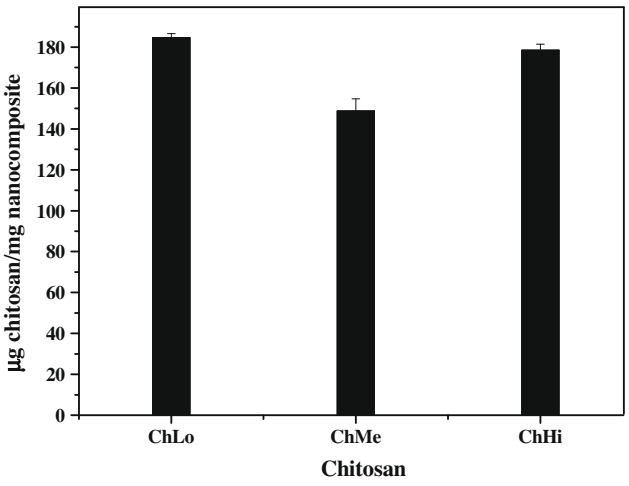

Fig. 2. Influence of molecular weight of chitosan on binding of chitosan to rectorite. Data labels: ChLo (20 kDa), ChMe (67 kDa) and ChHi (146 kDa).

with the highest and lowest molecular weight were chosen for further studies and their trimer substituted analogues were prepared (DS of 8.6% and 9.3%, respectively) as previously described (Tommeraas et al., 2002).

3.2. Structure and morphology of chitosan/rectorite nanocomposites

Fig. 3 shows the XRD patterns of rectorite and the nanocomposites, where the interlayer distances were obtained by Bragg's equation. Compared to pure rectorite, the d_{001} peaks of all the nanocomposites shift towards lower angle, which confirms the insertion of chitosan chains into rectorite. It can be seen that the interlayer distance depends on the content of chitosan; with increasing chitosan amount, the interlayer distance is larger. This is in agreement with a previous study (Wang et al., 2005), showing that the amount of intercalated chitosan in the interlayer of rectorite increased with increasing chitosan concentration. Furthermore, it can be observed that the interlayer distance is directly proportional to the molecular weight of chitosans. The shorter chains of the LMW chitosan facilitate the intercalation into rectorite. Similarly, unsubstituted chitosan can more easily enter into the interlayer of rectorite than the trimer-substituted chitosan. This is related to the size of the molecules; the free volume of substituted chitosan is larger than unsubstituted chitosan.

The internal structure of chitosan/rectorite nanocomposites is shown in Fig. 4 in two levels of magnification. The images exhibit typical morphology of the layered nanocomposites. The dark lines correspond to clay layers while the bright areas represent the chitosan matrix. From the lower magnification image (the left image), it could be observed that the silicate layers are dispersed well into the chitosan matrix at a nanometer scale despite the high content of clay (33.3 wt.%). A closer observation (the right image) reveal that the most of the silicate particles maintain the layered structure, and the interlayer distance of about 3 nm can be measured in TEM images, which agrees with the XRD analysis.

3.3. Size and colloidal stability of DNA-loaded nanocomposites and polyplexes

The mean hydrodynamic diameters (*z*-average) of the polyplexes and chitosan–DNA–rectorite nanocomposites are given in Fig. 5. Clearly, the size of polyplexes formed by different unsubstituted chitosans is close to the size of those formed by the trimer-substituted chitosans. When combining chitosans with rectorite, the size

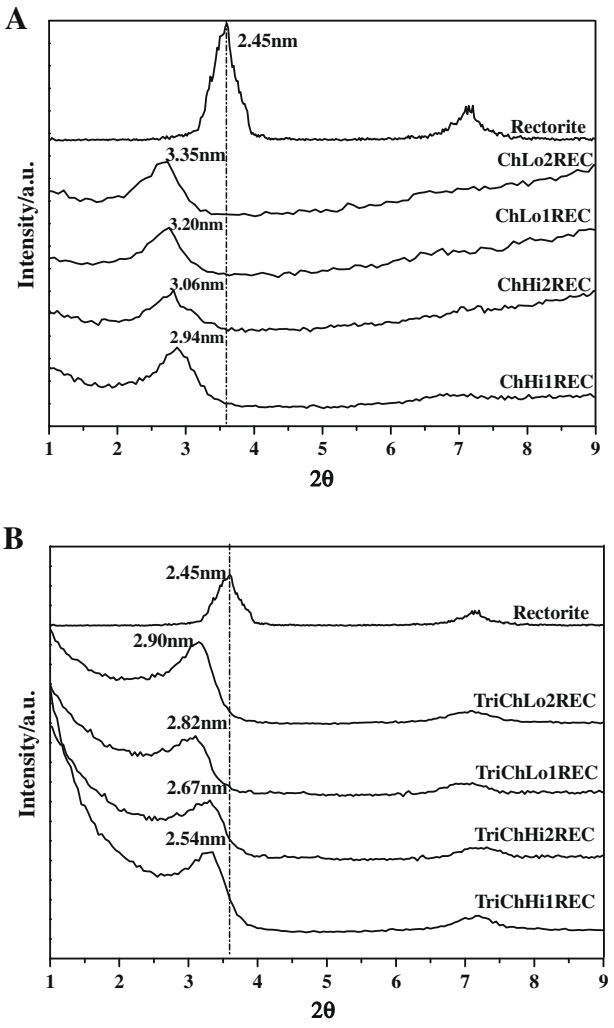

Fig. 3. XRD patterns of rectorite and chitosans/rectorite nanocomposites based on chitosan (A) and trimer-substituted chitosan (B). Description of nanocomposites is given in Table 2.

of the resulting nanocomposites increased compared to polyplexes and depended on the mass ratio between the chitosan and rectorite. The size of the nanocomposites decreased with increasing mass ratio of chitosan to rectorite from 1:1 to 2:1. A possible explanation is that at the higher ratio of chitosan to rectorite, there will be a lower tendency for aggregation of rectorite–chitosan particles due to their increased net positive charge.

The colloidal stability of polyplexes and chitosan–DNA–rectorite nanocomposites during transfection is also important in relation to their use as gene delivery vehicles. The aggregation of the non-stabilised polyplexes can influence the cellular uptake (Liu & Yao, 2002). Here, the aggregation kinetics of the polyplexes and chitosan–DNA–rectorite nanocomposites was studied in PBS at pH 7.4. As shown in Fig. 6, LMW chitosan/DNA polyplexes showed higher degree of aggregation than their HMW counterparts. The polyplexes formed by glycosylated chitosans were considerably more stable, confirming our previous studies (Issa et al., 2006; Strand et al., 2008). The substituted HMW chitosan formed the most stable polyplexes.

In addition, as shown in Fig. 6, rectorite/DNA mixtures *per se* were also aggregating. The rate of aggregation of chitosan–DNA–rectorite nanocomposites was affected both by the type of intercalated chitosan and its amount. It seems that DNA-loaded nanocomposites based on trimer-subtituted chitosans are more stable as

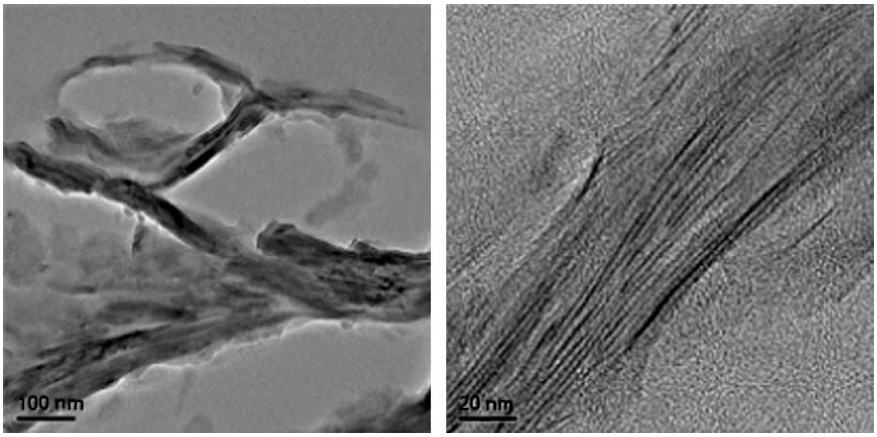

Fig. 4. TEM micrographs of ChLo2REC nanocomposite.

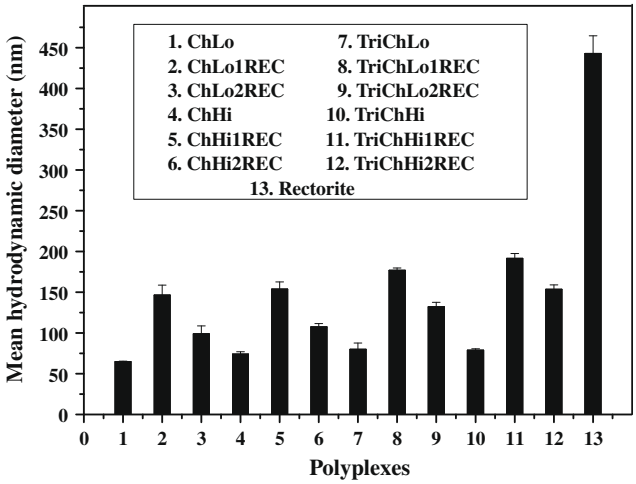

Fig. 5. Mean hydrodynamic diameters (*z*-average) of the chitosan–DNA polyplexes and chitosan–DNA–rectorite nanocomposites prepared at A/P 3 in MQ water. Description of chitosan and nanocomposites is given in Tables 1 and 2.

compared to those based on unsubstituted chitosans. Similarly as in case of polyplexes, inclusion of HMW chitosan was also favorable for colloidal stability.

3.4. DNA binding measured with the gel electrophoresis assay

The gel electrophoresis analysis was conducted to assess the binding capacity and stability of the complexes. To determine the stability of polyplexes and chitosan–DNA–rectorite nanocomposites as a function of the A/P ratio, different A/P ratios for each sample were tested. It can be seen from Fig. 7 that the stability of polyplexes varies considerably with the molecular weight of the chitosans and in combination with trimer-substitution, as previously observed (Issa et al., 2006). Generally, for polyplexes formed with fully deacetylated chitosans, the stability decreased with decreasing molecular weight and with trimer substitution. The complexes based on HMW chitosan and its trimer-substituted chitosan released DNA only at A/P ratio of 1 or lower, while the LMW chitosan/DNA complexes released DNA at A/P 3. The LMW trimer-substituted chitosan formed physically unstable polyplexes that released the pDNA even at such high A/P ratio as 10. This is in agreement with previous reports (Issa et al., 2006; Strand et al., 2005). Moreover, no difference between the stability of complexes

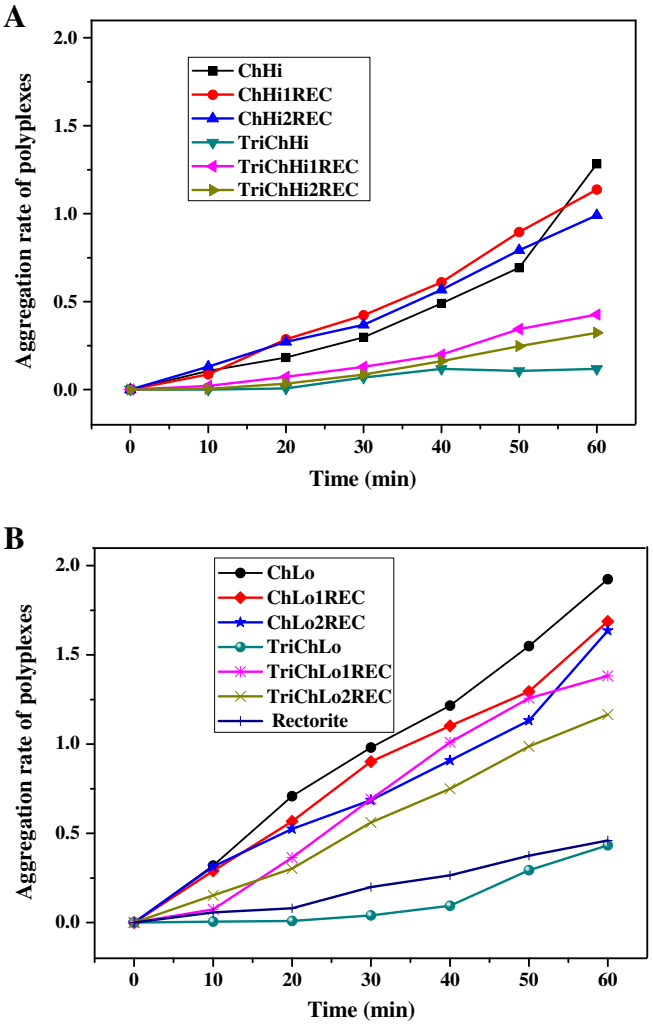

Fig. 6. Colloidal stability of polyplexes and chitosan–DNA–rectorite nanocomposites prepared at A/P 3 in PBS as a function of time. DNA–chitosan polyplexes and nanocomposites based on HMW chitosan (A) and LMW chitosan (B). The description of chitosan and nanocomposites is given in Tables 1 and 2.

based on HMW chitosan and the same chitosan substituted with trimer is found. However, when comparing the LMW chitosan with the same trimer-substituted chitosan, more unstable polyplexes are formed. The physical stability of the LMW chitosan-based com-

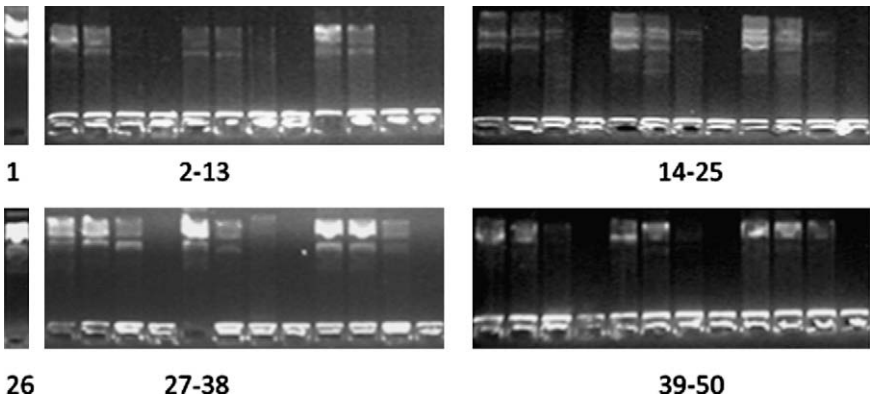

Fig. 7. Stability of the polyplexes and chitosan–DNA–rectorite nanocomposites in agarose gel electrophoresis assay. Polyplexes and nanocomposites were prepared in MQ water. The description of chitosan and nanocomposites is given in Tables 1 and 2. Lane 1: pDNA, l. 2–5: ChLo (A/P 0.5, 1, 3 and 5), l. 6–9:ChLo1REC (A/P 0.5, 1, 3 and 5), 10–13:ChLo2REC (A/P 0.5, 1, 3 and 5), 14–17: ChHi (A/P 0.3, 0.5, 1 and 3), 18–21: ChHi1REC (A/P 0.3, 0.5, 1 and 3), 22–25: ChHi2REC (A/P 0.3, 0.5, 1 and 3), 26: REC/pDNA, 27–30: TriChLo (A/P 3, 5, 10 and 20), 31–34: TriChLo1REC (A/P 10, 20, 30 and 60), 35–38: TriChLo2REC (A/P 3, 5, 10 and 20), 39–42: TriChHi (A/P 0.3, 0.5, 1 and 3), 43–46:TriChHi1REC (A/P 0.5, 1, 3 and 5), 47–50: TriChHi2REC (A/P 0.3, 0.5, 1 and 3).

plex is reduced by the trimer substitution, while the HMW chitosan/DNA complex is probably still too stable to be affected by the substitution.

As shown in Fig. 7, all DNA was released from rectorite/DNA complex, as expected. The stability of unsubstituted chitosan–DNA–rectorite nanocomposites is unaffected by rectorite. This is because pure rectorite is negatively charged, but after intercalation by chitosan, its surface charge is reversed. Thus, chitosan–DNA–rectorite nanocomposite retained DNA in a similar way as the polyplexes. However, in case of glycosylated chitosan, we observed an increased DNA release from the 1:1 nanocomposites compared to the polyplexes formed by the same chitosan. This effect is also consistent with the increased aggregation behavior of the same nanocomposites in PBS (Fig. 6). Stabilized nanocomposites based on

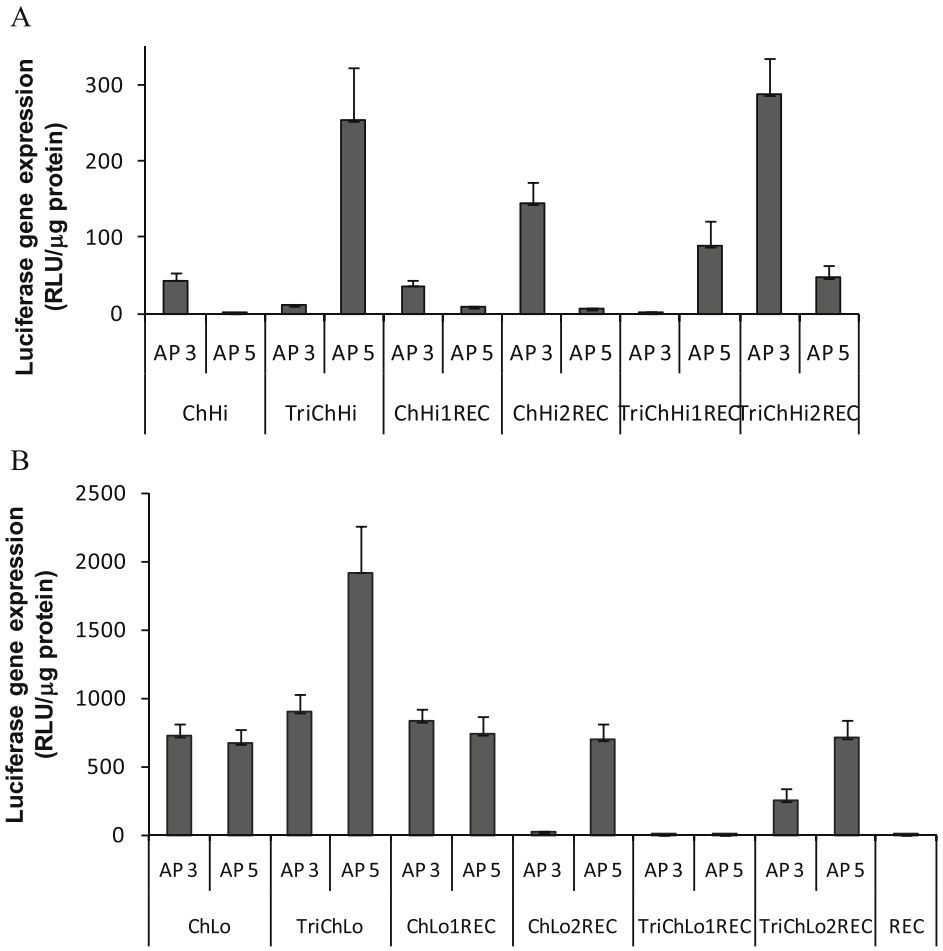

Fig. 8. In vitro gene transfection efficacy of chitosans and chitosans/rectorite nanocomposites with two different charge ratios (A/P 3 and 5). The results are presented as luciferase gene expression 72 h post transfection in RLU/μg of total cellular protein. Cells were transfected with 0.3 μg pDNA/well.

TriChLo1REC can only be obtained when the A/P ratios is increased to 60 (Fig. 7).

3.5. In vitro cell transfection

Transfection efficacy of chitosan–pDNA complexes and chitosan–pDNA–rectorite nanocomposites was evaluated in HEK293 cells. As shown in Fig. 8, LMW chitosans exhibited higher transfection efficacy than HMW chitosan, which is in agreement with other studies (Koping-Hoggard, Melnikova, Varum, Lindman, & Artursson, 2003; Strand et al., 2005). The trimer-substituted chitosans showed higher transfection efficacy than unsubstituted chitosans, in accordance with our previous study (Issa et al., 2006). Concerning the effect of rectorite, it seems that inclusion of rectorite in the formulation did not improve their in vitro transfection efficiency, which is unlike our previous study with quaternized chitosans in the human hepatocellular carcinoma cell line (HCCLM7) cell line (Wang, Pei, et al., 2008). This may reflect the differences in cell line, as the relative efficacy of gene delivery systems largely varies in different cell lines. Alternatively, the binding of trimethylated chitosan to the rectorite may reduce the toxicity of this chitosan derivative, thereby improving gene transfer efficacy.

4. Conclusions

The nanocomposites based on rectorite and four different chitosans (two fully deacetylated chitosans with low and high molecular weight and their glycosylated analogues) were successfully prepared and characterized. The interlayer distance of rectorite decreased with increasing molecular weight, the trimer substitution and decreasing the relative amount of chitosan. The DNA-loaded nanocomposites prepared from HMW chitosans showed higher colloidal stability and retention of DNA than those prepared from LMW counterparts. However, the polyplexes and nanocomposites containing the LMW and trimer-substituted chitosan showed highest gene delivery efficacy in HEK293 cells. Compared to conventional polyplex, chitosan–DNA–rectorite nanocomposites did not improve the transfection efficacy in this cell line.

References

Aguzzi, C., Cerezo, P., Viseras, C., & Caramella, C. (2007). Use of clays as drug delivery systems: Possibilities and limitations. *Applied Clay Science, 36*, 22–36.

Demaneche, S., Jocteur-Monrozier, L., Quiquampoix, H., & Simonet, P. (2001). Evaluation of biological and physical protection against nuclease degradation of clay-bound plasmid DNA. *Applied and Environmental Microbiology, 67*, 293–299.

Hashimoto, M., Morimoto, M., & Saimoto, H. (2006). Lactosylated chitosan for DNA delivery into hepatocytes: The effect of lactosylation on the physicochemical properties and intracellular trafficking of pDNA/chitosan complexes. *Bioconjugate Chemistry, 17*, 309–316.

Issa, M. M., Koping-Hoggard, M., Tommeraas, K., Varum, K. M., Christensen, B. E., Strand, S. P., et al. (2006). Targeted gene delivery with trisaccharide-substituted chitosan oligomers in vitro and after lung administration in vivo. *Journal of Controlled Release, 115*, 103–112.

Kawase, M., Hayashi, Y., Kinoshita, F., Yamato, E. Y., Miyazaki, J., Yamakawa, J., et al. (2004). Protective effect of montmorillonite on plasmid DNA in oral gene delivery into small intestine. *Biological & Pharmaceutical Bulletin, 27*, 2049–2051.

Kim, T. H., Jiang, H. L., Jere, D., Park, I. K., Cho, M. H., Nah, J. W., et al. (2007). Chemical modification of chitosan as a gene carrier in vitro and in vivo. *Progress in Polymer Science, 32*, 726–753.

Koping-Hoggard, M., Melnikova, Y. S., Varum, K. M., Lindman, B., & Artursson, P. (2003). Relationship between the physical shape and the efficiency of oligomeric chitosan as a gene delivery system in vitro and in vivo. *Journal of Gene Medicine, 5*, 130–141.

Koping-Hoggard, M., Varum, K. M., Issa, M., Danielsen, S., Christensen, B. E., Stokke, B. T., et al. (2004). Improved chitosan-mediated gene delivery based on easily dissociated chitosan polyplexes of highly defined chitosan oligomers. *Gene Therapy, 11*, 1441–1452.

Lin, F. H., Chen, C. H., Cheng, W. T. K., & Kuo, T. F. (2006). Modified montmorillonite as vector for gene delivery. *Biomaterials, 27*, 3333–3338.

Liu, K. H., Chen, S. Y., & Liu, D. M. (2008). Drug release behavior of chitosan–montmorillonite nanocomposite hydrogels following electro stimulation. *Acta Biomaterialia, 4*, 1038–1045.

Liu, S. Q., Peng, L., Yang, X. D., Wu, Y. F., & He, L. (2008). Electrochemistry of cytochrome P450 enzyme on nanoparticle-containing membrane-coated electrode and its applications for drug sensing. *Analytical Biochemistry, 375*, 209–216.

Liu, W. G., & Yao, K. D. (2002). Chitosan and its derivatives – A promising non-viral vector for gene transfection. *Journal of Controlled Release, 83*, 1–11.

Montier, T., Benvegnu, T., Jaffres, P. A., Yaouanc, J. J., & Lehn, P. (2008). Progress in cationic lipid-mediated gene transfection: A series of bio-inspired lipids as an example. *Current Gene Therapy, 8*, 296–312.

Ottøy, M. H., Vårum, K. M., & Smidsrød, O. (1996). Compositional heterogeneity of heterogeneously deacetylated chitosans. *Carbohydrate Polymers, 29*, 17–24.

Romoren, K., Pedersen, S., Smistad, G., Evensen, O., & Thu, B. J. (2003). The influence of formulation variables on in vitro transfection efficiency and physicochemical properties of chitosan-based polyplexes. *International Journal of Pharmaceutics, 261*, 115–127.

Strand, S. P., Danielsen, S., Christensen, B. E., & Varum, K. M. (2005). Influence of chitosan structure on the formation and stability of DNA–chitosan polyelectrolyte complexes. *Biomacromolecules, 6*, 3357–3366.

Strand, S. P., Issa, M. M., Christensen, B. E., Varum, K. M., & Artursson, P. (2008). Tailoring of chitosans for gene delivery. *Biomacromolecules, 9*, 3268–3276.

Tommeraas, K., Koping-Hoggard, M., Varum, K. M., Christensen, B. E., Artursson, P., & Smidsrod, O. (2002). Preparation and characterisation of chitosans with oligosaccharide branches. *Carbohydrate Research, 337*, 2455–2462.

Tommeraas, K., Varum, K. M., Christensen, B. E., & Smidsrod, O. (2001). Preparation and characterisation of oligosaccharides produced by nitrous acid depolymerisation of chitosans. *Carbohydrate Research, 333*, 137–144.

Usuk, I. A., Kawasum, I. M., Kojima, Y., Okada, A., Kurauchi, T., & Kamigaito, O. (1993). Swelling behavior of montmorillonite cation exchanged for w-amino acids by e-caprolactam. *Journal of Material Research, 8*, 1174–1178.

Varum, K. M., Anthonsen, M. W., Grasdalen, H., & Smidsrod, O. (1991). Determination of the degree of N-acetylation and the distribution of N-acetyl groups in partially N-deacetylated chitins (chitosans) by high-field n.m.r. spectroscopy. *Carbohydrate Research, 211*, 17–23.

Viseras, C., Aguzzi, C., Cerezo, P., & Bedmar, M. C. (2008). Biopolymer–clay nanocomposites for controlled drug delivery. *Materials Science and Technology, 2008*(24), 1020–1026.

Wang, X. Y., Du, Y. M., & Luo, J. W. (2008). intercalated nanoparticles: Preparation and controlled-release property. *Nanotechnology, 19*, 065707.

Wang, X. Y., Pei, X. F., Du, Y. M., & Li, Y. (2008). A new polymer/clay intercalative material for gene delivery system. *Nanotechnology, 19*, 375102.

Wang, S. F., Shen, L., Tong, Y. J., Chen, L., Phang, I. Y., Lim, P. Q., et al. (2005). Biopolymer chitosan/montmorillonite nanocomposites: Preparation and characterization. *Polymer Degradation and Stability, 90*, 123–131.

Yuan, W. Y., Ji, J., Fu, J. H., & Shen, J. C. (2008). A facile method to construct hybrid multilayered films as a strong and multifunctional antibacterial coating. *Journal of Biomedical Materials Research, 85B*, 556–563.

Yuan, Q., Venkatasubramanian, R., Hein, S., & Misra, R. D. K. (2008). A stimulus-responsive magnetic nanoparticle drug carrier: Magnetite encapsulated by chitosan-grafted-copolymer. *Acta Biomaterialia, 4*, 1024–1037.

Zeng, Q. H., & Yu, A. B. (2008). Molecular dynamics simulations of organoclays and polymer nanocomposites. *International Journal of Nanotechnology, 5*, 277–290.